

# CURRENT STATUS OF THE ADVANCED RESIDUAL GAS MONITOR FOR HEAVY ION SYNCHROTRON APPLICATIONS\*

D.Liakin<sup>#</sup>, V.I.Skachkov, S.Barabin, O.Sergeeva (ITEP, Moscow), P.Forck, T.Giacomini (GSI, Darmstadt), V.I.Skachkov, A.Vetrov (MSU, Moscow), A.Paal (MSL, Stockholm).

## Abstract

The challenge and complexity of the advanced RGM requires very careful design of each structural component and special attention to match the properties of different subsystems. In the present paper the status of the high performance readout electronics is discussed. Single optical decoupled profile measurement channel (one of 100) with 14 bit resolution and 10 MHz bandwidth was tested and step-by-step improved. Special attention had been paid to the noise cancellation and digital data processing algorithms optimization.

Another important point is a proper electromagnetic guiding system design. As it is shown, high field homogeneity, which is required for sub-mm spatial resolution, can be achieved despite the presence of the field distorting hole for the light signal transmitting. The low energy (down to 10MeV per nucleon) beam disturbance compensation methods are also discussed. The ionization process and electron dynamics simulations are used for proving this system design.

## THE STATUS OF THE FAST PROFILE READOUT ELECTRONICS

The advanced RGM structure was described in details in [1] and [2]. It will cover profile measurements with 0.1 microseconds of time and 1mm spatial resolution. A phosphor coated Microchannel Plate (MCP) is proposed as a wide bandwidth high resolution primary detector. A bundle of 100 optically decoupled from the signal source digitizing channels will allow fast measurement option in addition to the slow profile measurements with a CCD camera. Avalanche photodiode (APD) is used as a light receiver to provide required bandwidth, sensitivity and dynamic range. The saturating of the MCP output basically limits the signals level, therefore low noise operation is mandatory [3]. The structure of the data acquisition channel is shown in Fig. 1.

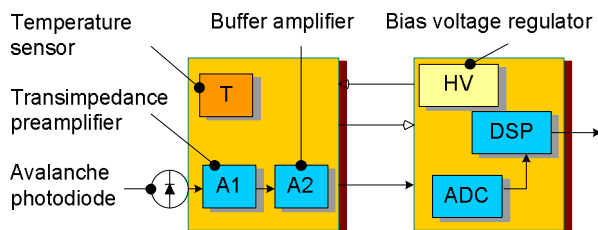


Figure 1: The structure of one photodiode readout channel

A two-module structure was chosen to build a compact, EMI protected head with embedded photodiode and to

connect it to a more sophisticated data processing module. To diminish an induced noise and EMI a two-stage preamplifier (A1 and A2) is placed in the head. The sensor T provides the APD temperature which is then used by a digitally controlled high voltage source (HV) to fix the APD multiplication factor. A 14 bits 65MHz ADC sampling rate exceeds the Nyquist frequency, which reduces the requirements to the analog antialiasing filter.

The test setup consists of the readout channel itself, a wide bandwidth LED emitter fed by a signal generator, Hamamatsu's wide band optical receiver and personal computer for control and data presentation. A serial connection was used to communicate with the PC. A dedicated control software had been designed for the DSP and PC to provide a suitable Windows interface with graphical output. A real-time data filtering and decimation algorithms were implemented in C code for fast on-line data processing in the DSP. Three frequency bands were used to cover full frequency range of further applications.

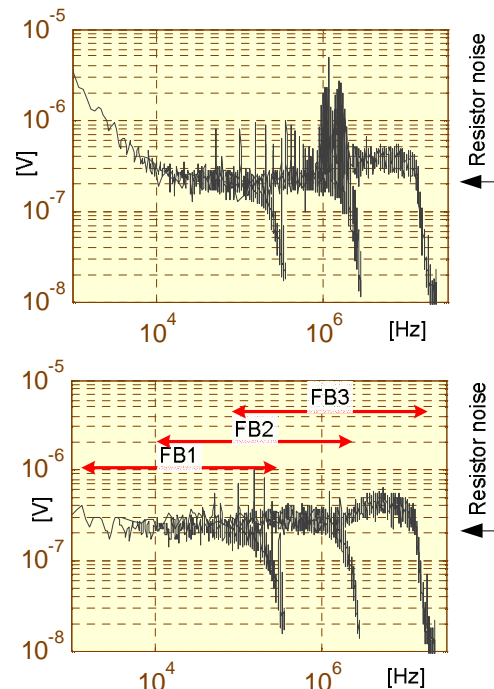


Figure 2: Preamplifier output noise (amplified) before (on the top) and after optimisation

To measure the frequency response of the readout channel the noising properties of the avalanche photodiode were used. The shot noise of a photodiode grows like square root of DC current or incoming light intensity, therefore an illuminated APD can be interpreted as a white noise generator. This APD feature was used to

\*Work supported by INTAS, Reg.No.:03-54-3931

<sup>#</sup>liakin@itep.ru

obtain the frequency response-like spectrum on the amplifier's output.

At the design phase the computer simulation was used to define the estimated output voltage noise on the first stage preamplifier's (A1) output. This simulation gives the value of  $40 \text{ nV/Hz}^{1/2}$  of the noise power density for the medium frequency range and increases this value for higher frequencies due to the dropping of the operational amplifier gain. The medium frequency range noise consists mainly of the feedback resistor thermal noise and hence can be considered as the lowest achievable theoretical value. The next design phase was dedicated to analysing and suppressing of all extra noise sources. On the top of figure 2 one can see the measured noise spectrum, which still includes a number of external spectrum lines. Some of these lines may be identified with switching power supplies, PC monitor or microprocessor clock frequencies. A few printed board geometries and power supply configurations were tested before the suitable result was obtained. This figure shows the noise spectrum during and after the design optimisation. The resulting noise spectrum is quite similar to the one obtained by the computer simulation.

As it was mentioned above, three frequency regions were used to cover the full frequency range of the future application. The highest frequency band is limited by an antialiasing analog 13 MHz filter while the other two are limited by performing a digital filtering in the DSP. The filtering and decimation of the incoming data were executed as real-time operations by DSP in the data processing module. The performance of the DSP was tested in advance to define the maximum achievable quality of digital filtering. In this test mode the data was acquired by DSP by embedded direct memory access channel. Two switching data banks in the internal DSP memory were used for data reception and evaluation. The required processor time for filtering and decimation was directly measured by a scope and compared to the incoming data rate (acquisition time). As a result, an 80 taps FIR structure has been accepted for the decimation filters of the frequency bands 1 and 2.

### ELECTRON DYNAMICS TO MCP

In RGMs an electrostatic field accelerates the ionization products of the beam and residual gas towards a MCP. The fast readout option of our project requires a short drift time and therefore electrons should be used for profile imaging. To compensate the space charge effect and electrons initial velocity spread a guiding uniform magnetic field is applied to allow precise electron positioning on the MCP surface. Detailed requirements to the E and B-fields strength and uniformity were presented in [2]. 100 mT B-field and 50 kV/m E-field are required to cover all proposed RGM applications at GSI. To achieve the desired resolution, the 100 mT magnetic field provides an average cyclotron radius of the electrons smaller than 0.1 mm, as demonstrated in Fig. 3(a). Fig. 3(b) shows the 1D probability  $P_y$  as a function of

sweep argument  $y$ ; more than 65 % of the generated electrons hit the circle with radius of 0.1mm.

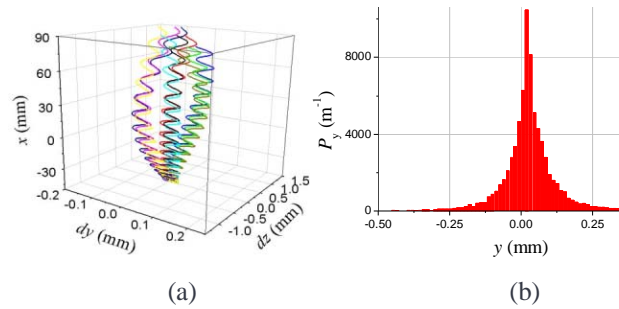


Figure 3: Electron trajectories – (a) and (b) – integrated distribution at MCP along sweep direction.

The RGM resolution is very sensitive to the orthogonal magnetic field component. To limit the electron deflection with the desired value, this component should be decreased below 0.2 % of the field magnitude. The beam-coincident magnetic field projection is allowed to deviate up to several percents of the field magnitude without affecting the monitor accuracy.

To simulate the ionization process we used a simple model of two interacting point charges. By our code we integrated the electron dynamic equations in the field of a moving ion. After ionization the daughter products (one free electron and one residual gas ion) interact with the external magnetic and electric fields generated by RGM systems and the electromagnetic field generated by the beam.

To present the bunch field the 3D Gaussian charge distribution was used. During electron dynamic calculations toward the MCP our code takes into account the bunch motion up to relativistic velocities.

### RGM CHANNELS

#### E-Field:

A dipole box design with side electrodes supplied with linearly changed potential is used for electric field generation.

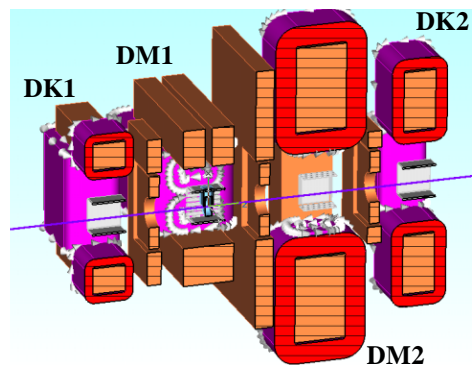


Figure 4: RGM magnetic & electric channels elevation.

Such dipole even of 200 mm long at  $\varnothing 180 \text{ mm}$  aperture provides acceptable field uniformity. A voltage of  $\pm 4.52 \text{ kV}$  is applied to the bottom and the top electrodes establishing field strength of about 50 kV/m. The main

dipoles are supplemented with a pair of correcting dipoles seen in Fig. 4 to compensate the electric field kick even it is much smaller than magnetic one. Adjacent electric dipoles do not influence each other though steel plates installed into the vacuum chamber for magnetic shielding described below give simultaneously electric shielding reducing electric field superposition.

**B-Field:**

The magnetic channel shown in Fig. 4 consists of two main dipoles DM1 and DM2, two dipoles DK1 and DK2 for kick compensation, and three steel shields arranged along  $z$ -axis. The channel sizes are: square of  $1024 \times 1024 \text{ mm}^2$  transversely and 2175 mm longitudinally, at an aperture of  $481 \times 481 \text{ mm}^2$ . The main dipoles and correctors are of “window frame” design. This design provides required accuracy of the field configuration and possibility to assemble/disassemble the dipoles from the beam pipe for high temperature vacuum bake out.

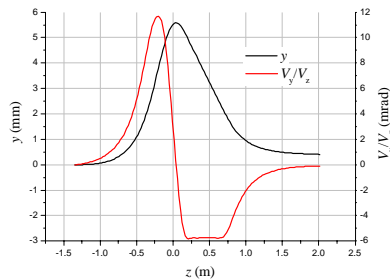


Figure 5: Kick compensation.

We extracted the beam image light from the MCP screen through the slit in the poles of the main dipoles. These 40 mm wide slits are cut-through the whole pole width to reduce magnetic field disturbance near the MCP. A small ratio between the magnet length and the aperture size and a limited permeability of the real steel lead to the field distortion, which we had to neutralize by additional small-power coils attached to the main windings on both sides of the vacuum chamber.

The monitor's  $E$  and  $B$  fields result in a transverse kick up to 10 mrad or greater for lower energy ion beam. Beam perturbations should be compensated by magnets with the same field configuration. Such correctors have two pairs of coils exciting both transverse field components. Such channel solution provides transverse kick compensation both in horizontal and vertical planes seen in Fig. 5.

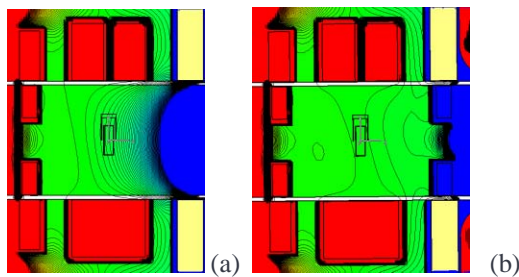


Figure 6: Sweep direction field component without (a) and with (b) internal steel shield.

We optimised the geometry and potential distribution of correctors to reduce the ion beam shift and its velocity inclination at the channel output down to 1 mm and 1 mrad and smaller.

To shrink the length of the RGM we separated each of two working regions by special steel plates installed between pairs of adjacent dipoles. Practically it was necessary to place some parts of these shields with an aperture hole of  $\varnothing 180 \text{ mm}$  just inside the vacuum chamber. Fig. 6 shows the shielding of the second monitor dipole field penetration into the first dipole working region ( $10^{-4} \text{ T}$  distance between adjacent isolines).

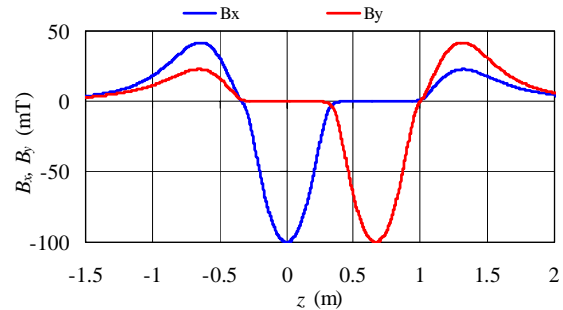


Figure 7: Transverse magnetic field distribution.

As seen in Fig. 7 our channel has symmetric field  $x$ - and  $y$ -distributions with required 100 mT in the working region centres and practically suppressed parasitic components on each dipole length.

**CONCLUSIONS**

The application of an external magnetic field increases both the monitor resolution and detection rate. Our monitor, which is able to operate at two mode regimes, was developed to provide beam diagnostics of any ion types in very wide ranges of ion energy and intensity.

*Acknowledgments*

The authors are grateful to professor B. Sharkov for encouragement at the monitor design development.

**REFERENCES**

- [1] P. Forck et al. Development of a Permanent Magnet Residual Gas Profile Monitor With Fast Readout, in Proc. DIPAC 2003, p. 134, Mainz, Germany, <http://accelconf.web.cern.ch/accelconf/d03/papers/P17.pdf>
- [2] T. Giacomini et al, “Development of a residual gas profile monitor with high resolution and fast readout”, in Proc. BIW04, Knoxville, Tennessee May 3-6, 2004. <http://www.sns.gov/biw04/>
- [3] D. Liakin et al. Development of a Permanent Magnet Residual Gas Profile Monitor With Fast Readout, in Proc EPAC2004, p. 2724, Lucerne, Switzerland, <http://accelconf.web.cern.ch/accelconf/e04/PAPERS/THPLT100.PDF>